11th International Symposium on Turbulence and Shear Flow Phenomena (TSFP11)
Southampton, UK, July 30 to August 2, 2019

THREE-DIMENSIONAL FLOW STRUCTURES AROUND A FINITE WALL-MOUNTED CYLINDER CONTROLLED BY USING AN INCLINED HOLE

Hiroka Rinoshika, Akira Rinoshika
Department of Mechanical Systems Engineering
Yamagata University
4-3-16 Jonan, Yonezawa-shi, Yamagata 992-8510, Japan
rinosika@yz.yamagata-u.ac.jp

Xiao-Lei Han, Hang-Yu Zhu, Cheng-Yue Wang, Jin-Jun Wang
School of Aeronautic Science and Engineering
Beijing University of Aeronautics and Astronautics
37 Xueyuan, Haidian District, Beijing 100191, China
jjwang@buaa.edu.cn

ABSTRACT
Three-dimensional flow structures around a finite wall-mounted cylinder, which is drilled an inclined hole going from the rear surface to the top surface inside a circular cylinder of an aspect ratio 1 (RIH), are instantaneously measured by Tomographic PIV in a water tunnel. Here both of the diameter D and height H of circular cylinder are 70 mm. Tomographic PIV measurement was performed at Reynolds number of 8,570 in a water tunnel. Three dimensional time-mean velocity fields, vorticity and Q criterion are discussed and compared between the hole and no hole of low-aspect-ratio cylinders. It is found that RIH generates a stronger counter-rotating vortex pair near the free end and a stronger downwash flow behind the RIH cylinder. Comparing to the standard cylinder, the arch vortex and large-scale vortices break down slowly in the wake of RIH cylinder.

INTRODUCTION
A finite circular cylinder makes a strongly three-dimensional complex flow structure, and the aspect ratio (the ratio of the height and diameter) of the cylinder influences the wake flow, which is different from the structure of an infinite circular cylinder (Rinoshika and Zhou, 2005, 2009), due to the effect of the free end (or tip) of the cylinder and the connection of cylinder and wall (Sumner et al., 2004; Pattenden et al., 2005; Wang and Zhou, 2009; Goncalves et al., 2015). The engineering field has many important applications, such as reducing drag and noise induced by designing the offshore structures, heat exchangers, structural vibrations, automobile and so on. The investigation of the complex flow structures of the finite circular cylinder can be found a lot. Kármán vortex from the both sides of the cylinder, the horse shoe vortex (called necklace vortex) and base vortex near the ground of the connection of the cylinder and wall (Tanaka and Murata, 1999; Sumner et al., 2004) and a pair of streamwise counter-rotating vortices (called trailing vortices) generating from the free end (Kawamura et al., 1984a; Johnston and Wilson, 1996; Adaramola et al., 2006) can be observed. Lee (1997) also informed that a structure like Kármán vortex cell is reduced related to the aspect ratio when the aspect ratio is high. The tip-vortices (Okamoto and Yagita, 1973; Kawamura et al., 1984b; Roh and Park, 2003) and a horse shoe vortex (Krajnović, 2011; Rostamy et al., 2012) exist around a low-aspect-ratio cylinder, while alternating vortex shedding, i.e., Kárman street, can't be found. At the case of a lower-aspect-ratio cylinder, "arch-type vortex" formation appears in the near wake (Lee, 1997) because the vortex from the free-end surface is influenced by the vortices generated from the sides before reattaching to the ground. The details about finite-height cylinder can be seen in Sumner (2013) and Porteous et al. (2014). Recently，Zhu et al. (2017) used tomographic PIV to measure the three-dimensional flow structures around a short wall-mounted cylinder with an aspect ratio of 2, and found the instantaneous 3D M-shape arch vortex.

However little investigation focuses on controlling vortices in the short cylinder wakes. Recently, Rinoshika et al. (2017) developed a passive control method, in which an inclined hole drilled from the rear surface to the free-end surface is used to control the flow around a short cylinder. It was found that the lengths of rear separation region are effectively reduced. Furthermore, Rinoshika et al. (2018) drill a horizontal hole from the surface of front side to the surface of rear side inside the short cylinder to generate the jet flow, which reduced the area of the rear separation region effectively. One of important purpose in the flow control is generally to suppress the vortices or the rear circulation zone in the wake. However, how the flow issued from the inclined hole effects on three-dimensional flow structures behind the short cylinder is yet unclear, which motivates the present investigation.

In order to clarify three dimensional wake flow structures around low-aspect-ratio cylinders with the hole and no hole on the flat plate, Tomographic PIV is used to measure instantaneously the three dimensional velocity fields in a water tunnel. Three dimensional velocity fields, vorticity and Q criterion are discussed and compared between the hole and no hole of low-aspect-ratio cylinders.

EXPERIMENTAL SETUP AND MEASUREMENT METHOD
The experiment was conducted in a circular open water tunnel. The size of the test section is 3000 mm (length) x 600 mm (width) x 700 m (height). As shown in Figure 1(a), a short circular cylinder with a height of H =70mm and a diameter of D = 70 mm (the aspect ratio of H/D = 1) is mounted on a flat plate. Inside the cylinder, as shown in Fig.1(b), a hole with a diameter of d = 10 mm (d/D=0.14) is drilled from the rear surface to the free end surface, called rear inclined hole (RIH).

For evaluating the effect of the hole height, we use three RIH models with different hole positions on the rear side surface (h = 20mm, 35mm and 50mm), expressed as RIH20, RIH35 and RIH50, respectively. Here the centre of the hole on the surface of free end is fixed at L=30mm from the leading edge of cylinder (Rinoshika et al., 2017).

The circular cylinder model was mounted on the central axis of the bottom wall 1200 mm downstream of the test section entrance. The streamwise, spanwise and wall-normal directions were indicated by the x, y, and z axes, respectively. A free stream velocity is fix at U = 0.162 m/s, corresponding to Reynolds number Re ($\equiv UD/\nu$) of 8,570. The origin of the coordinate system was set at the centre of the cylinder bottom surface.

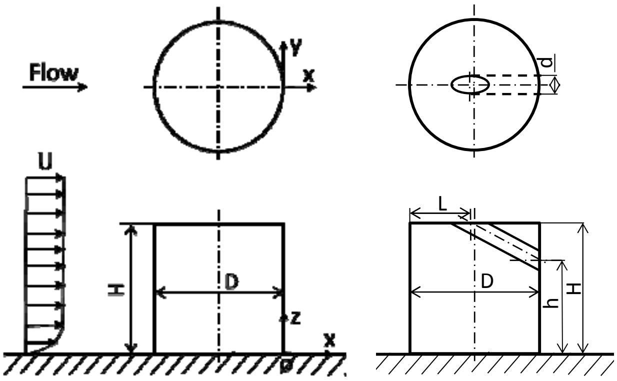

(a) Standard cylinder (b) RIH cylinder

Fig.1 Short circular cylinder models

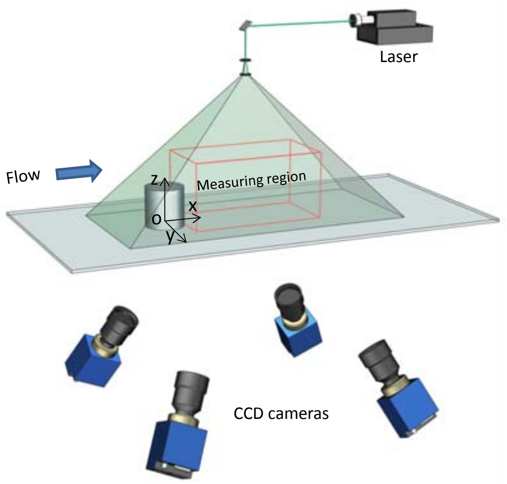

Fig.2 Tomographic PIV setup

The experimental apparatus for the tomographic PIV measurements is shown in Fig.2. The PIV tracer particles with a mean diameter of 10 μm are adopted. Illumination was provided by a dual-head Nd:YAG laser (500 mJ/pulse, 532 nm wavelength) with a pulse separation time of 3 ms, which yields average displacements of approximately 0.48 mm (8 pixels) in the free-stream region. The optical lenses and the mirror were designed to generate an 80 mm thick light sheet illuminating the tracer particles around the cylinder. The light sheet was perpendicular to the test section bottom. Four high-resolution (6600 x 4400 pixels^2, 12bit) double-exposure CCD cameras (IMPERX SM-CCDB29M2) were applied to record the measurement domain simultaneously. In Fig.2, the viewing angles were approximately 47 between cameras. The measurement volume was in the coordinate range [-115; 130], [-70; 70], [0; 100] (mm) with a digital imaging resolution of 0.075 mm per pixel, so that its corresponding physical domain had a size of 245 x 140 x 100 mm^3. Tomographic particle image velocimetry (TPIV) was applied in the present investigation for its ability to display the average and instantaneous three-dimensional distribution of velocity and vorticity. The 3D vector calculation was done through multi-pass correlation analysis with a deforming interrogation window. In the final pass, the interrogation volume was 32 x 32 x 32 voxel with 50% overlap, leading to a spatial resolution of 2.4 mm and a vector pitch of 2.4 mm.

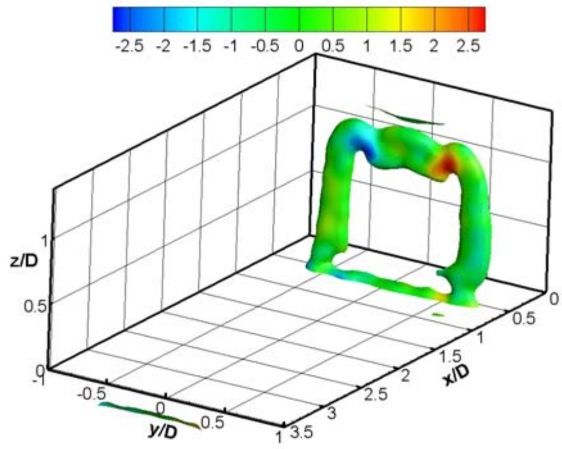

(a) no hole

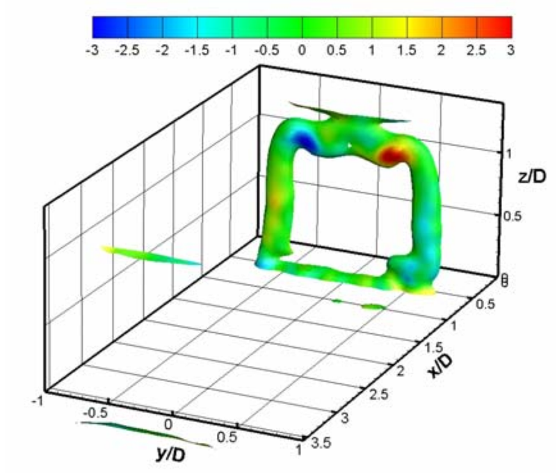

(b) RIH cylinder with h = 0.5D

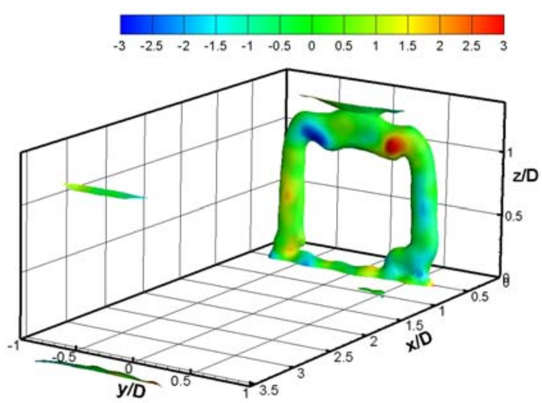

(c) RIH cylinder with h = 0.71D

Fig.3 The mean isosurface of $Q/(U/D)^2$=5 colored by the streamwise vorticity $\overline{\omega}_x D/U$

RESULTS AND DISCUSSION

Fig. 3 shows the mean isosurface of $Q/(U/D)^2=5$ colored by the streamwise vorticity $\overline{\omega}_x D/U$ around the standard and RIH (with h = 0.5D, 0.71D) cylinders. As shown in Fig.3(a), the arch vortex structure of standard cylinder clearly exhibits a W-type head instead of a reversed U (Lee, 1997) or an M shape (Zhu et al., 2017) standing on the ground plane behind the short cylinder. Two concave parts near the two sides of the horizontal part are evidently observed in the W-type arch structure, which is caused by the downward flow from the free end and tip vortex. The center convex of the horizontal part on the W-type arch structure is induced owning to the strong upwash effect of the large flow separation behind the short cylinder. Being different from M-sharp arch structure (Zhu et al., 2017), the larger distance between two tip vortices results in the weaker effect of tip vortices on center part of the head even though they have strong vorticity at the two sides of the arch head. At the case of RIH cylinders, W-type head of arch structures becomes weaker and closes to reversed U shape. It is because that a part of upwash flows through the rear side surface hole and the effect of upwash flow on the arch strcture becomes weaker. Two concave parts near the two sides of the horizontal part becomes smaller due to the effect of stronger issue flow from the hole of the free end surface.

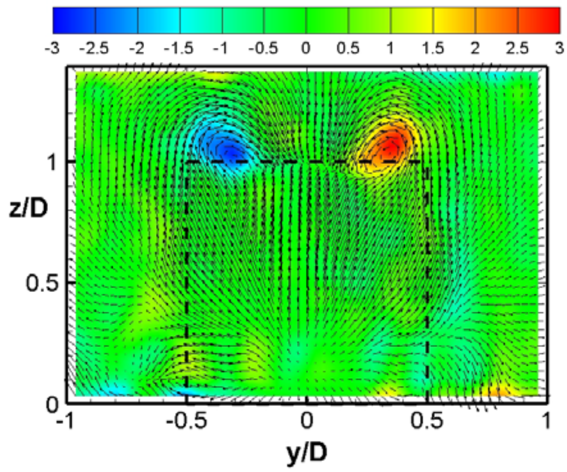

(a) Standard cylinder

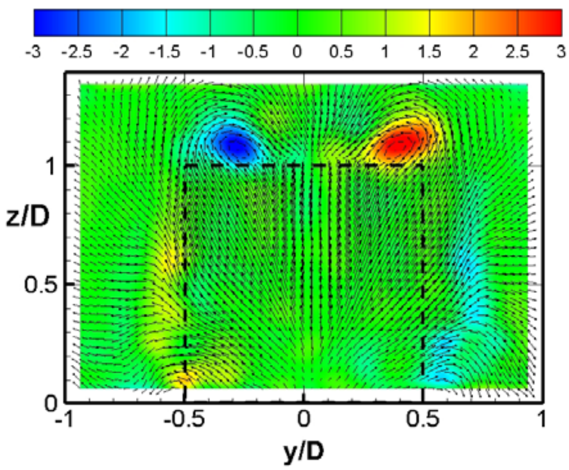

(b) RIH cylinder with h = 0.5D

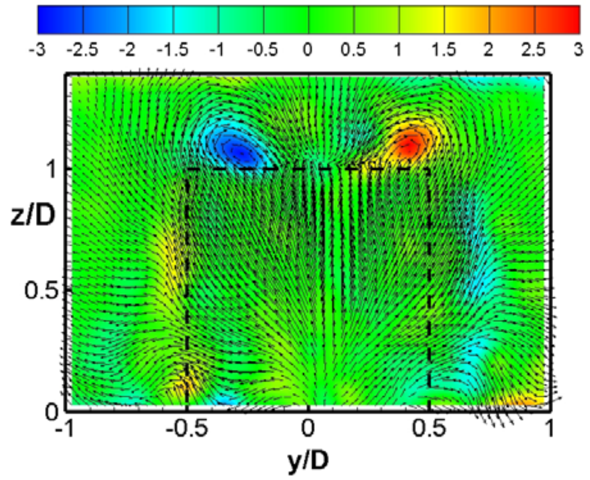

(c) RIH cylinder with h = 0.71D

Fig.4 The mean velocity vectors with the contour of the mean streamwise vorticity $\overline{\omega}_x D/U$ in the (y, z)-plane of x/D=0.7

Fig. 4 shows the distribution of mean velocity vectors with the contour of the mean streamwise vorticity $\overline{\omega}_x D/U$ around the standard and RIH (with h = 0.5D, 0.71D) cylinders in the (y, z)-plane at the downstream of x/D=0.7. As found by Rinoshika et al. (2017), the fluid of the large rear recirculation zone flows upwards to small recirculation zone of the free end surface through the RIH. At the location of x/D=0.7, a pair of tip vortices can be clearly observed in the standard cylinder wake. The upwash and downwash flows can be seen between two tip vortices near the top surface the cylinder, which is an important reason forming the W-type head of arch structure in the short cylinder wake. At the case of RIH cylinders, the position of tip vortices become higher, and the distance between them becomes wider than that of the standard cylinder due to the effect of the issue flow from the hole on the free end surface. As the height of the side hole increases, the distance and the height of the two tip vortices slightly increase because the streamwise velocity of issue flow from the hole on the free end surface increases.

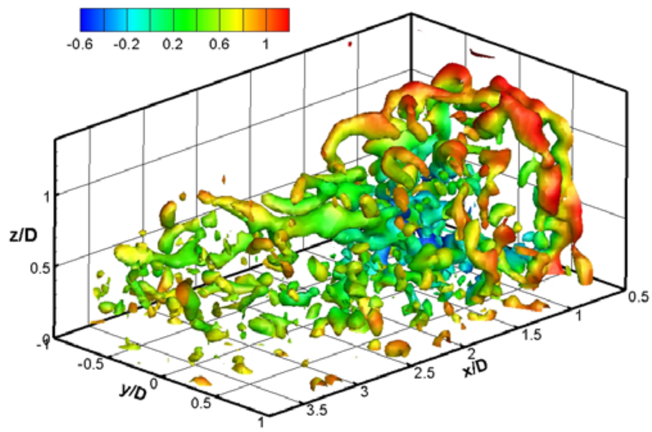

(a) Standard cylinder ($Q/(U/D)^2$=13.5)

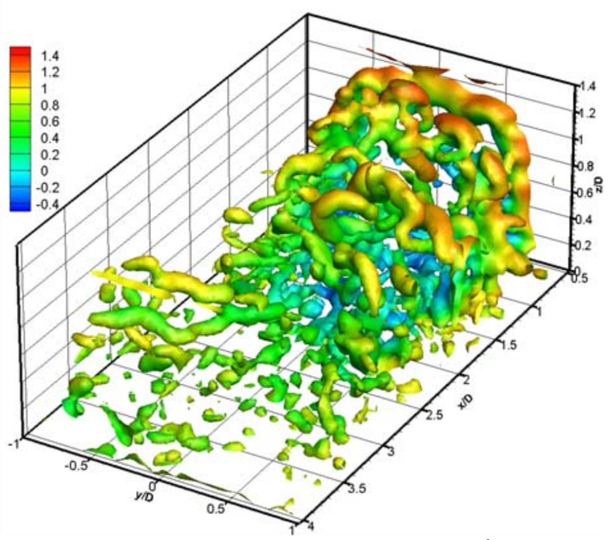

(b) RIH cylinder with $h = 0.5D$ ($Q/(U/D)^2$=5)

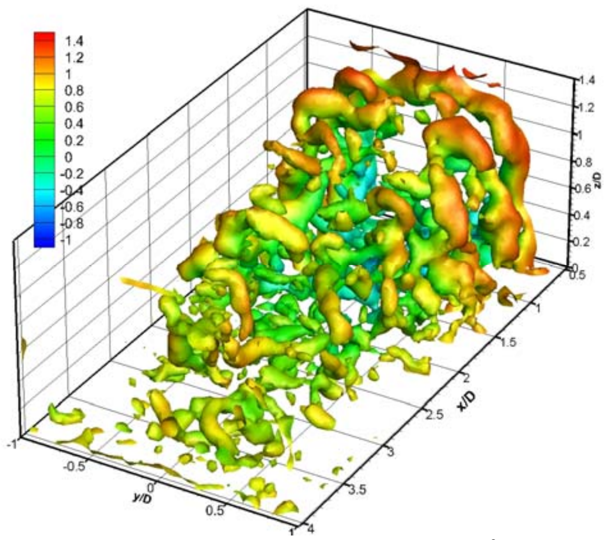

(c) RIH cylinder with $h = 0.71D$ ($Q/(U/D)^2$=5)

Fig.5 Instantaneous isosurface of $Q/(U/D^2)$ colored by the velocity u/U

Fig.5 shows the instantaneous isosurface of $Q/(U/D^2)$ colored by the velocity u/U around the standard and RIH (with h = 0.5D, 0.71D) cylinders. Three-dimensional vortical structures of various scales, such as the arch vortex, tip vortex and the large-scale streamwise vortex, are clearly observed. The free end originates the top flow separation and tip vortices at the trailing edge, which induces a W-shape arch vortex. The center convex of the horizontal part of the W-type arch structure is produced due to the upwash effect of the large flow separation behind the cylinder. The two concave parts of the horizontal part are caused by the downward flow and tip vortices. At the case of hole cylinders, the large-scale arch vortex and large-scale streamwise vortex close to the cylinder are clearly observed The W-shape of the head becomes slightly weaker due to the effect of the suction flow from the side hole on the upwash flow from the flat plate. The issue flow also results in decreasing two concave parts in the horizontal part of arch structure. Comparing with the standard cylinder, the arch vortex and large-scale vortices break down slowly.

Conclusions

To clarify the three-dimensional flow structures behind a wall-mounted short cylinder with the hole and no hole, the Tomographic PIV measurements are carried out in this study. The main results are shown as follows.

(1) The W-shape head becomes weaker at the case of the hole models.
(2) At the case of RIH cylinders, the tip vortices become strong, and the distance between them becomes larger.
(3) As the height of the hole increases, the distance and the height of the tip vortices also increase.
(4) 3D various scale vortical structures can be observed behind the models.
(5) Comparing with standard cylinder, the arch vortex and large-scale vortices break down slowly.

REFERENCES

Adaramola, M.S., Akinlade, O.J., Sumner, D., Bergstrom, D.J., Schenstead, A.J., 2006, Turbulent wake of a finite circular cylinder of small aspect ratio, Journal of Fluids and Structures, Vol.22, pp.919–928.

Gonçalves, R.T., Franzini, G.R., Rosetti G.F., Meneghini, J.R., Fujarra, A.L.C., 2015, Flow around circular cylinders with very low aspect ratio, Journal of Fluids and Structures, Vol.54, pp.122–141.

Johnston, C.R., Wilson, D.J., 1996, A vortex pair model for plume downwash into stack wakes, Atmospheric Environment, Vol.31, pp.13–20.

Kawamura, T., Hiwada, M., Hibino, T., Mabuchi, T., Kumada, M., 1984a, Flow around a finite circular cylinder on a flat plate, Bulletin of the JSME, Vol.27, pp.2142–2150.

Kawamura, T., Hiwada, M., Hibino, T., Mabuchi, T., Kumada, M., 1984b, Flow around a finite circular on flat plate: in the case of cylinder length larger than turbulent boundary layer thickness, Transactions of the JSME, Vol.50, pp.332–341. (in Japanese).

Krajnović, S., 2011, Flow around a tall finite cylinder explored by large eddy simulation, Journal of Fluid Mechanics, Vol.676, pp.294–317.

Lee, L.W., 1997, Wake structure behind a circular cylinder with a free end, In: Proceedings of the Heat Transfer and Fluid Mechanics Institute, pp. 241–251.

Okamoto, T., Yagita, M., 1973, The experimental investigation on the flow past a circular cylinder of finite length placed normal to the plane surface in a uniform stream, Bulletin of the JSME, Vol.16, pp.805–814.

Pattenden, R.J., Turnock, S.R., Zhang, X., 2005, Measurements of the flow over a low-aspect-ratio cylinder mounted on a ground plane, Experiments in Fluids, Vol.39, pp.10-21.

Porteous, R., Moreau, D.J., Doolan, C.J., 2014, A review of flow-induced noise from finite wall-mounted cylinders, Journal of Fluids and Structures, Vol.51, pp.240–254.

Rinoshika, A., Zhou, Y., 2005, Orthogonal wavelet multi-resolution analysis of a turbulent cylinder wake, Journal of Fluid Mechanics, Vol.524, pp.229-248.

Rinoshika, A., Zhou, Y., 2009, Reynolds number effects on wavelet components of self-preserving turbulent structures, Physical Review E, Vol.79, 046322, pp.1–11.

Rinoshika, H., Rinoshika, A., 2018, "Effect of a horizontal hole on flow structures around a wall-mounted low-aspect-ratio cylinder", International Journal of Heat and Fluid Flow, Vol. 71, pp.80–94.

Rinoshika, H., Rinoshika, A., Fujimoto S., 2017, “Passive control on flow structure around a wall-mounted low aspect ratio circular cylinder by using an inclined hole”, Bulletin of the JSME, Journal of Fluid Science and Technology, Vol. 12, pp.1-13.

Rinoshika, H., Rinoshika, A., Fujimoto S., 2018, “Visualization of a finite wall-mounted cylinder wake controlled by a horizontal or inclined hole”, Journal of Visualization, Vol. 21, pp. 543-556.

Roh, S.C., Park, S.O., 2003, Vortical flow over the free end surface of a finite circular cylinder mounted on a flat plate, Experiments in Fluids, Vol.34, pp.63–67.

Rostamy, N., Sumner, D., Bergstrom, D.J., Bugg, J.D., 2012, Local flow field of a surface-mounted finite circular cylinder, Journal of Fluids and Structures, Vol.34, pp.105-122.

Sumner, D., 2013, Flow above the free end of a surface-mounted finite-height circular cylinder, A review, Journal of Fluids and Structures, Vol.43, pp.41-63.

Sumner, D., Heseltine, J.L., Dansereau, O.J.P., 2004, Wake structure of a finite circular cylinder of small aspect ratio, Experiments in Fluids, Vol.37, pp.720–730.

Tanaka, S., Murata, S., 1999, An investigation of the wake structure and aerodynamic characteristics of a finite circular cylinder, JSME International Journal, Series B: Fluids Thermal Engineering, Vol.42, pp.178–187.

Wang, H.F., Zhou, Y., 2009, The finite-length square cylinder near wake, Journal of Fluid Mechanics, Vol.638, pp.453–490.

Zhu H. Y., Wang C. Y., Wang H. P. and Wang J. J., 2017, “Tomographic PIV investigation on 3D wake structures for flow over a wall-mounted short cylinder”, Journal of Fluid Mechanics, Vol. 831, pp. 743-778.